

Light Scattering and Electrical Conductivity Studies of the Aerosol OT Toluene Water–In–Oil Microemulsions

M. Mercedes Velázquez,^{*,†} Margarita Valero,[‡] and Francisco Ortega[§]

Departamento de Química Física, Facultad de Química, Universidad de Salamanca, Plaza de la Merced s/n, 37008 Salamanca, Spain, Departamento de Química Física, Facultad de Farmacia, Universidad de Salamanca, Apdo. 449, 37080 Salamanca, Spain, and Departamento de Química Física I, Facultad de Ciencias Químicas, Universidad Complutense, 28040 Madrid, Spain

Received: August 2, 2000; In Final Form: July 23, 2001

By using electrical conductivity and static and dynamic light scattering measurements, the behavior of water–oil (w/o) microemulsions formed by Aerosol OT dissolved in toluene has been examined. To study the effect of the droplet volume fraction on the microemulsion behavior, the water and the surfactant concentrations were systematically modified and the temperature dependence was also studied. The scattering intensity and the apparent diffusion coefficients are analyzed with a model involving the Carnahan–Starling hard-sphere model including an attractive term. It was found that attractive interactions become important in w/o microemulsions containing $w_0 > 37$. No percolation threshold is detected at the droplet volume fraction and temperature values used in this work.

Introduction

Microemulsions are thermodynamically stable, isotropic transparent dispersions of two immiscible liquids, i.e., water and hydrocarbon, and one or more surfactants. A water–oil (w/o) microemulsion contains isolated water pools surrounded by a monolayer of surfactant molecules dispersed in a continuous oil phase. AOT as surfactant is well-known to form w/o microemulsions in several alkane oils. The aggregation process is fairly well characterized with respect to size and shape at various water contents.^{1–5} All of these works concluded that the w/o microemulsion structure primarily depends on the water/surfactant molar concentration ratio, $w_0 = [\text{water}]/[\text{surfactant}]$, and on the bulk solvent.^{6–9}

In previous papers, we reported structural properties of AOT w/o microemulsions dissolved in cyclohexane, isooctane, and toluene and we also studied the effect of the addition of water-soluble polymers on the structure and properties of these microemulsions.^{9–12} Infrared and fluorescence spectroscopy, dynamic light scattering, and conductivity measurements were used. Results showed significant differences between the water structure of AOT microemulsions dissolved in toluene and those dissolved in cyclohexane and isooctane.⁹ On the other hand, the electrical conductivity results shown that in microemulsions composed of AOT dissolved in toluene conductivity increases until a certain critical w_0 value, around 25–35, and above this water concentration, a sharp increase of the conductivity was observed.¹⁰ However, this increase of conductivity is not sharp enough to attain the percolation threshold. The addition of poly(vinylpyrrolidone) and poly(sodium-4-styrenesulfonate) polymers prevents this behavior.¹⁰ The breakpoint of conductivity/water concentration curves was also observed in the photophysical properties of Acridone solubilized in these microemulsions.¹³

It is well established that AOT forms in toluene w/o microemulsions.¹⁴ The size and the aggregation number of these microemulsions have been determined by dynamic light scattering and viscosity measurements.⁸ Results indicate that at relatively low water concentration, $w_0 \leq 10$, the droplet radius linearly increases with w_0 . Significant differences between results obtained by dynamic light scattering and viscosity were observed. In all cases, the radii obtained by DLS were lower than those measured by viscosity method, differences were interpreted as being due to polydispersity.⁸ The linear relation between the droplet radius and w_0 was observed in AOT microemulsions dissolved in some organic solvents.⁸ However, by using synchrotron radiation small-angle X-ray scattering, some deviation from the linear relation were detected in apolar solvents such as *n*-hexane, *n*-heptane, *n*-octane, and isooctane.^{15,16} Recently,¹⁷ using small angle neutron scattering (SANS), the radius of microemulsions of D₂O/AOT/C₆D₅CD₃ without and with additives has been reported for $w_0 \leq 20$. Neglecting interdroplet interactions, these results show that at low water content ($w_0 \leq 7$) the radius linearly increases with w_0 , whereas at $w_0 \approx 7.5$, a sharp increase of the droplet radius is reported; however, above this water content, the radius increases. When additives are present, the droplet radius is smaller and a slight change with w_0 is observed. There are no results of the size of AOT toluene w/o microemulsions containing a water concentration greater than 20.

Geiger reported that the maximum water concentration solubilized in these microemulsions was $w_0 = 12$ at 298 K and that increasing the water content leads to a phase separation.¹⁸ We will show in this work that stable microemulsions containing until $w_0 = 50$ can be prepared.

In this work, we are interested in the origin of the sharp increase of conductivity of AOT toluene w/o microemulsions containing high water concentrations. Therefore, by using dynamic light scattering, we determine the effect of water and surfactant concentrations on the droplet size. In addition, the effect of the temperature on the behavior of these w/o micro-

* To whom correspondence should be addressed. Fax: 00-34-923-294574. E-mail: mvsal@usal.es.

[†] Facultad de Química, Universidad de Salamanca.

[‡] Facultad de Farmacia, Universidad de Salamanca.

[§] Universidad Complutense.

emulsions is also studied. Simultaneously, we used the electrical conductivity method to detect the presence of percolation process.

Experimental Section

Materials and Samples Preparation. Sodium bis(2-ethylhexyl)sulfosuccinate, AOT, was from Fluka. It was purified according to the published method.¹⁹ After the sample was dried, some water molecules remain bound to the AOT. The residual water concentration of the AOT/toluene stock solutions was analyzed with a Karl-Fisher titration, and this water concentration was taken into account in the w_0 calculation. Spectroscopic grade toluene was purchased from Fluka and was stored in sodium. Water was treated with a Milli-Q system from Millipore.

To study the effect of the water concentration on the microemulsion structure, w_0 was modified between 15 and 50, and up to this w_0 value, a cloudy solution appears at 298.15 K. The surfactant concentration has also been systematically modified from 0.05 to 0.15 M. Microemulsions were prepared by adding the appropriate amount of water to the corresponding stock solution of AOT in toluene and stirring until the solution became transparent. The incorporation of water was carried out by the successive addition of a small volume of water to the stock surfactant solutions. When the microemulsions contain high water concentration, the solubilization process needs several days.

Conductivity Measurements. The electrical conductivity was measured at different temperatures using a CDM 83 conductometer from Radiometer, Copenhagen, which operates at 73 Hz, and an Ingold low-conductivity cell of $0.0822 \pm 0.0004 \text{ cm}^{-1}$. The constant of the cell was obtained by calibration with KCl solutions of known concentrations.²⁰ The temperature was controlled by means of a thermostat/cryostat RM 6 B from LAUDA.

Light-Scattering Measurements. Static and dynamic measurements were performed with a Malvern apparatus using the green line ($\lambda = 514.5 \text{ nm}$) of an argon ion laser (Coherent I300). The correlator (Malvern K 7032) is equipped with 256 channels.

Dynamic light scattering measurements were performed at six different scattering angles between 30 and 140°. All of our experiments showed single-exponential correlation functions, and the data were analyzed by using a second-order cumulants fit.²¹ The first and second cumulants, k_1 and k_2 , yield the relaxation rate, k_D , of the autocorrelation function $k_1 = k_D = D_m q^2$, and the variance, $v = k_2^2/k_1$, related to the polydispersity of the system, where D_m is the apparent diffusion coefficient, and q is the scattering wave vector, $q = (4\pi n \sin^{1/2}\theta)/\lambda$, where λ is the wavelength in a vacuum, n is the refractive index of the medium, and θ is the scattering angle. In all cases, the relaxation rate is linear with q^2 . For spherical particles, the apparent diffusion coefficient is related to the apparent hydrodynamic radius, R_h^{app} , by the Stokes–Einstein relation: $D_m = k_B T / (6\pi\eta R_h^{\text{app}})$, where T is the absolute temperature, k_B is Boltzmann's constant, and η is the viscosity of toluene at a given temperature.²²

Static light scattering experiments were performed at 23 different angles ($30^\circ < \theta < 140^\circ$), and 20 individual measurements were taken and averaged for each angle. The absolute scattering intensity, I , was calculated using toluene as reference standard by

$$I = \langle I(\theta) \rangle / \langle I_{\text{ref}}(\theta) \rangle \quad (1)$$

where $\langle I(\theta) \rangle$ and $\langle I_{\text{ref}}(\theta) \rangle$ are the average excess scattering intensity of the solution and the average scattering intensity of the solvent toluene, respectively. No dependence of the scattering intensity with the scattering angle was observed.

Values of the refractive index for AOT dissolved in toluene with different water concentrations were measured with a DRA1 refractometer from Atago. To remove dust particles, solutions were filtered before measurements with Millipore 0.2 μm filters. The scattering cell was thermostated within $\pm 0.1^\circ\text{C}$, and the temperature was measured with a calibrated Pt-100 sensor.

Results and Discussion

Conductivity Measurements. It is well-known that the conductivity of water-in-oil microemulsions changes with the water concentration. At higher water content, the conductivity is comparable to that of electrolyte solutions. However, at lower water concentration, the drop conductivity sharply decreases by 3–4 orders of magnitude because of the percolation threshold.^{23–26} Percolation can be also induced at constant water volume fraction by increasing the temperature. In both cases, the electrical conductivity measurements are routinely used for detecting the percolation threshold.^{24,27–30} Below the percolation threshold, the conductivity decreases with decreasing the volume fraction of water, but its order of magnitude is still much higher than the solvent conductivity. This higher conductivity of w/o microemulsions has been explained by the charge fluctuation model.³¹ This model considers that the charged droplets are formed by a spontaneous number of fluctuations of the ions contained on the droplets. The magnitude of these fluctuations is related to the Coulomb energy required to charge up the droplet.³¹ According to this model, the conductivity of a dilute microemulsion, κ , can be expressed by

$$\kappa = \epsilon_0 \epsilon k T \phi / 2\pi \eta r^3 \quad (2)$$

where ϵ_0 is the dielectric permittivity of the vacuum, ϵ is the dielectric constant of the solvent, r is the droplet radius, and ϕ is the volume fraction of drops: $\phi = (V_{\text{water}} + V_{\text{AOT}}) / (V_{\text{water}} + V_{\text{AOT}} + V_{\text{toluene}})$.

To detect the presence of percolation in AOT/toluene w/o microemulsions, we analyze the electrical conductivity at constant temperature of microemulsions containing different volume fraction of drops. To obtain the associated surfactant concentration and volume of AOT, we use $\text{cmc} = 0.016 \text{ M}$. This value was determined by fluorescence by using Acridone as probing.³²

Figure 1 presents the results corresponding to w/o microemulsions with AOT concentrations of 0.08 and 0.1 M and variable w_0 at 298.15 K. In the figure, the specific conductivity, κ/ϕ , is represented as a function of ϕ . As can be seen in the figure, specific conductivity is approximately constant until $\phi \approx 0.065$, (AOT = 0.08 M and $w_0 = 25$) and $\phi \approx 0.1$ (AOT = 0.1 M and $w_0 = 35$). In both cases, at $\phi > 0.1$ and $w_0 \geq 35$, the conductivity sharply increases. The regime of constant specific conductivity has been identified with dilute water-in-oil microemulsions.³¹ The weak ϕ dependence at this region has been interpreted as caused by Coulombic as well as short-range interactions between droplets themselves.³¹ On the other hand, the sharp increase of specific conductivity is not high enough to show evidences of percolation. This agrees with results reported in the literature.³³ No percolation was observed in AOT toluene reverse microemulsions with $w_0 = 11.2$, whereas the

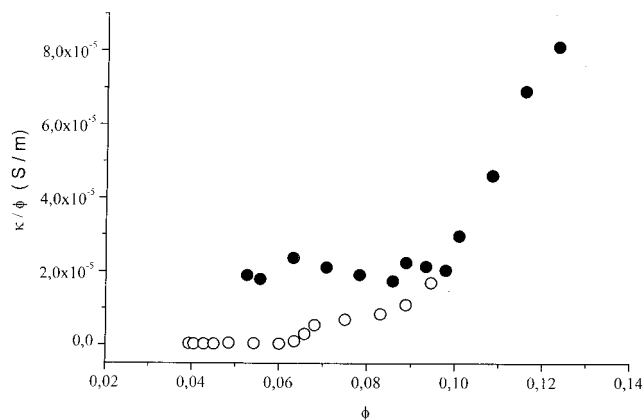


Figure 1. Variation of the specific conductivity, κ/ϕ , with the droplet volume fraction of w/o microemulsions of AOT dissolved in toluene: open circles [AOT] = 0.08 M and filled circles [AOT] = 0.1 M.

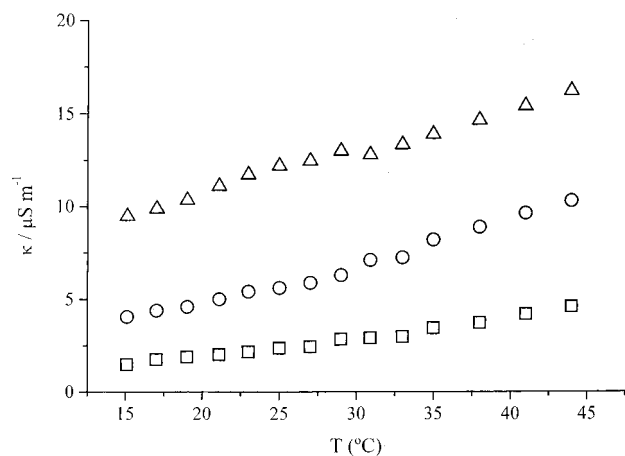


Figure 2. Temperature dependence of the electrical conductivity of AOT/toluene w/o microemulsions containing different droplet volume fractions: squares $\phi = 0.083$; circles $\phi = 0.109$; and triangles $\phi = 0.123$.

TABLE 1: Activation Energy Calculated from Conductivity and Dynamic Light Scattering Measurements of AOT/Toluene w/o Microemulsions with $w_0 = 40$, as a Function of the Droplet Volume Fraction

[AOT]/M	ϕ	$E_{a\text{cond}}/$ kJ mol ⁻¹	$(E_{a\text{DLS}})^a/$ kJ mol ⁻¹
0.08	0.083	27.4	19.9
0.10	0.109	24.9	17.0
0.12	0.134	13.9	20.2

^a Values determined by dynamic light scattering, see text.

addition of acrylamide or acetonitrile induces the percolation phenomena in such microemulsions.³³

The conductivity of microemulsions formed by constant volume fraction at different temperatures was also determined. Three different droplet volume fractions, below, above, and at $\phi = 0.1$, were selected, whereas the water concentration remains constant, $w_0 = 40$. Figure 2 presents these conductivity values. From the figure, no percolation was observed in the whole range of temperatures studied (between 15 and 44 °C).

The energy of activation for conductivity can be estimated³⁴ from the $\ln \kappa$ vs $1/T$ plot according to the Arrhenius equation $\kappa = Ae^{-E_a/RT}$. A linear relation is obtained in all cases. As an illustrative example, Figure 3 presents some of these data. Values of the energy of activation from conductivity are summarized in Table 1.

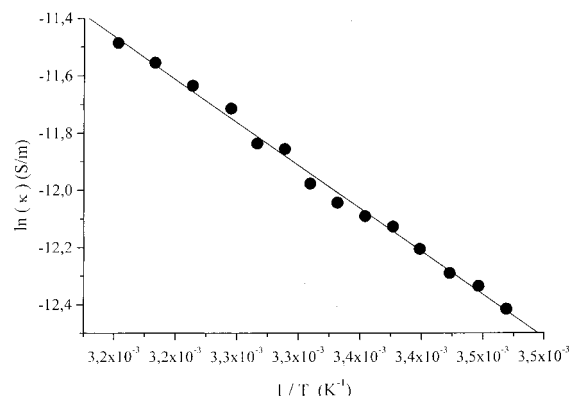


Figure 3. Arrhenius plot of $\ln \kappa$ vs $1/T$ corresponding to w/o microemulsions of AOT dissolved in toluene containing $w_0 = 40$ and [AOT] = 0.10 M.

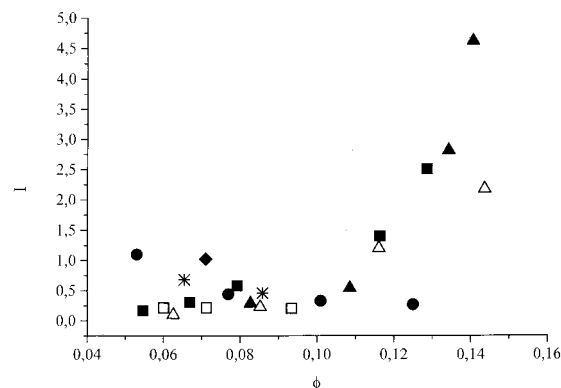


Figure 4. Light scattering intensity values as a function of the droplet volume fraction of w/o microemulsions of AOT dissolved in toluene: diamond $w_0 = 15$; star $w_0 = 25$; open squares $w_0 = 30$; circles $w_0 = 35$; filled squares $w_0 = 37$; filled triangles $w_0 = 40$; open triangles $w_0 = 45$.

The energy of activation for percolating systems has been reported in the literature.^{34–37} They can be low or high depending on the weak or strong percolation character but are always greater than 100 kJ/mol. The values found in this work are always lower than 100 kJ/mol confirming that the percolation threshold is not reached in this system at the droplet volume fractions studied. The values of Table 1 also show that the energy of activation decreases as ϕ increases. This fact indicates a more open structure³⁷ when the droplet volume fraction increases. The behavior is more accentuated at the droplet volume fraction $\phi = 0.134$.

Conductivity results indicate that the droplet volume fraction 0.1 seems to be a critical value. Above this droplet volume fraction, the sharp increase of conductivity could be due to droplets structural changes or pretransitional effect. To elucidate this behavior, we have performed light scattering measurements.

Static Light Scattering Measurements. The light scattering intensity was measured on microemulsions containing different water and surfactant concentrations. The intensity was found independent of the scattering angle in all of the solutions studied. The values corrected for background, cell and solvent, are represented in Figure 4 as a function of ϕ . These results show that for microemulsions with $w_0 \leq 35$ the scattering intensity decreases on increasing the volume fraction. Although, for microemulsions with $w_0 \geq 37$, the scattering intensity initially increases with ϕ and goes through a maximum around $\phi \approx 0.13$. It was not possible to prepare microemulsions with $\phi > 0.15$ because phase separation takes place in these systems. To

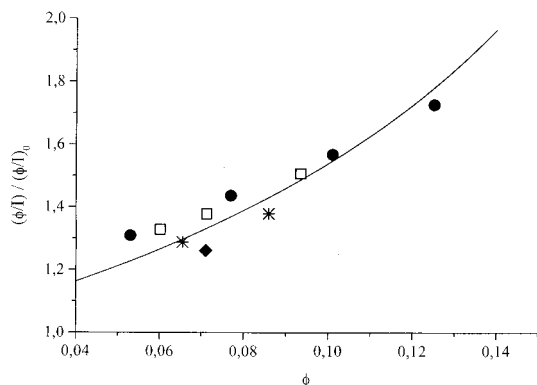


Figure 5. Variation of the inverse structure factor, $(\phi/I)/(\phi/I)_0$, as a function of the volume fraction of water droplets for AOT/toluene microemulsions: $w_0 = 15$ (diamond); $w_0 = 25$ (star); $w_0 = 30$ (open squares); and $w_0 = 35$ (circles). The line is the theoretical fit to eq 5.

rationalize this behavior, we consider two different regimes: aggregates with small water concentration and with high water contents.

The scattered intensity can be expressed as³⁸

$$I(q) = k\phi P(q) S(q) \quad (3)$$

where k is a constant, ϕ is the volume fraction, $P(q)$ is the intraparticle form factor, and $S(q)$ the structure factor. Because the observed scattered intensity is constant with q , it can be safely assumed that $P(q) = P(0) = 1$ and that $S(q)$ can be approached by the $q = 0$ limit, $S(0)$, that can be written as

$$S(0) = 1 - k_s\phi \quad (4)$$

where the concentration coefficient, k_s , depends on the pair interaction potential energy and adopts the value $k_s = 8$ for a pure hard sphere potential. The inverse structure factor can be expressed as

$$S(0)^{-1} = (\phi/I)/(\phi/I)_0 = (1 - k_s\phi)^{-1} \quad (5)$$

Figure 5 shows the variation of $S(0)^{-1}$ with ϕ in the small water concentration regime, $15 \leq w_0 \leq 35$, and the fit to eq 5 gives a k_s value of 3.5 ± 0.2 , smaller than the one corresponding to the hard sphere limit. This value can be explained because an attractive contribution to the pair interaction potential, which will be shown later to be very important for microemulsion with $w_0 > 37$. It is worth mentioning that both the value of k_s and the curvature of the plot is a clear indication that the usual approximation³⁹ $(1 - k_s\phi)^{-1} \approx (1 + k_s\phi)$ does not hold for the ϕ range spanned in Figure 5.

Figure 6 shows the variation of the scattered intensity with ϕ for microemulsions containing $w_0 \geq 37$. As it can be seen in the figure, the scattering intensity passes through a maximum around volume fraction 0.13. This behavior is classical for concentrated hard sphere systems.⁴⁰ We use the empirical Carnahan–Starling formula for the osmotic pressure of a hard-sphere system; this equation is known to fit nicely both simulation and experimental data:

$$\Pi_{\text{HS}} = (k_B T/V_{\text{HS}})[\phi + \phi^2 + \phi^3 - \phi^4]/(1-\phi)^3 \quad (6)$$

where $V_{\text{HS}} = 4/3\pi R_{\text{HS}}^3$. Accordingly, to conductivity results, we also consider an attractive potential V_A . If this potential is small, it is usually treated as a perturbation, and the contribution to

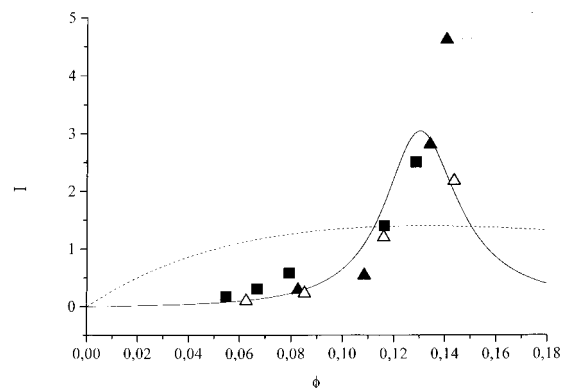


Figure 6. Scattering intensity as a function of the volume fraction of water droplets for AOT/toluene microemulsions: squares $w_0 = 37$; filled triangles $w_0 = 40$; and open triangles $w_0 = 45$. The solid curve is the theoretical fit to eq 9. The dotted line is calculated with the Carnahan–Starling model, see text.

TABLE 2: Apparent Diffusion Coefficients of AOT Toluene Microemulsions Obtained from Dynamic Light Scattering Measurements

W_0	[AOT]/ M	ϕ	$D_m/$ $10^{10} \text{ m}^2/\text{s}$	W_0	[AOT]/ M	ϕ	$D_m/$ $10^{10} \text{ m}^2/\text{s}$
15	0.10	0.071	2.24	37	0.11	0.116	2.20
25	0.08	0.065	2.40	37	0.12	0.129	2.03
30	0.08	0.071	2.60	40	0.08	0.083	3.87
30	0.10	0.093	3.10	40	0.10	0.109	2.68
35	0.06	0.053	2.03	40	0.12	0.134	1.83
35	0.08	0.077	2.58	40	0.125	0.141	1.78
35	0.10	0.100	2.81	45	0.08	0.089	4.10
35	0.12	0.125	3.44	45	0.09	0.103	1.95
37	0.07	0.067	2.21	45	0.10	0.116	2.60
37	0.08	0.079	2.48	45	0.12	0.144	2.16
37	0.09	0.092	1.91	50	0.10	0.124	1.41

the osmotic pressure Π_A is given by⁴¹

$$\Pi_A = (k_B T/2V_{\text{HS}})A\phi^2 \quad (7)$$

where the constant A determines the strength of the attractive potential.

Taking into account that the scattering intensity is proportional to the isothermal osmotic compressibility⁴²

$$I = G (\delta n/\delta \phi)^2 \phi N k_B T (\delta \pi/\delta \phi)^{-1} \quad (8)$$

where G is a constant independent of the sample and $(\delta n/\delta \phi)$ was calculated for each series with w_0 constant; thus, it can be deduced that

$$I = B'\phi[(1 + 4\phi + 4\phi^2 - 4\phi^3 + \phi^4)/(1-\phi)^4 + A\phi]^{-1} \quad (9)$$

Here B' is an experimental constant.

The solid line in Figure 6 represents the best theoretical fit with eq 9 and $B' = 0.57 \pm 0.03$ and $A = -21 \pm 4$. The dotted line represents the best fit with $A = 0$, only hard-sphere model without attractive potential. As can be seen, only the hard-sphere model cannot predict this behavior. The value found for the parameter A indicates that in this system attractive interactions become important when w_0 increases.

Dynamic Light Scattering Results. Dynamic light scattering measurements were also performed at different water contents, w_0 , and surfactant concentrations. The relaxation rate was obtained from the first cumulant at different scattering wave vectors. In all cases, the inverse relaxation rate shows a linear

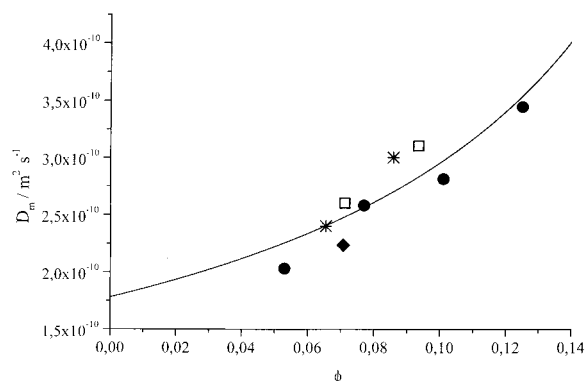


Figure 7. Variation of the apparent diffusion coefficient as a function of the droplet volume fraction of w/o microemulsions of AOT dissolved in toluene: diamond $w_0 = 15$; star $w_0 = 25$; open squares $w_0 = 30$; circles $w_0 = 35$. The line was calculated with eq 12.

dependence on q^2 , and from the slope, the apparent diffusion coefficient is obtained. The experimental D_m values are collected in Table 2. The diffusion coefficient values show a behavior consistent with the light scattering intensity data. For the microemulsions with $15 \leq w_0 \leq 35$, D_m shows an increase with the volume fraction, ϕ . This variation can be understood using the $q \rightarrow 0$ limit of Ackerson⁴³ relation for the diffusion coefficient:

$$D(q \rightarrow 0) = [D_0/S(0)][1 + H(0)] \quad (10)$$

D_0 corresponds to the droplet translational diffusion coefficient at infinite dilution from which the hydrodynamic radius, R_h , can be obtained using the Stokes–Einstein relation. The perturbation $H(0)$ arises from flow-related interactions, and at the simple level, it can be expressed as⁴⁴

$$H(0) \approx k_H \phi \quad (11)$$

Combining eqs 5, 10, and 11 we have

$$D_m = D_0(1 + k_H \phi)/(1 - k_S \phi) \quad (12)$$

The fit to all of the diffusion coefficient data found for microemulsion with $15 \leq w_0 \leq 35$, Figure 7, gives an average D_0 value of $(1.8 \pm 0.1) \cdot 10^{-10} \text{ m}^2 \text{ s}^{-1}$, corresponding to a hydrodynamic radius of $\sim 2.2 \text{ nm}$. The values obtained for the concentration coefficients k_S and k_H are 4 ± 0.6 and 0 within the error, respectively. The k_S value is in agreement with the one found from intensity data in the same w_0 range. The k_H value indicates that hydrodynamic interactions are negligible, although this result may be a consequence of the lack of precision of data in Figure 7 and/or a partial cancellation between the static and the hydrodynamic terms.

For microemulsions with $w_0 > 37$, the diffusion coefficients show a minimum at a volume fraction around 0.13 that coincide with the maximum found for the scattered intensity. Intermediate values are observed for $w_0 = 37$, and in this case, the apparent diffusion coefficient practically remains constant with ϕ . To explain the $w_0 > 37$ results, we used eq 10 together with the relation between the $q \rightarrow 0$ limit of the static structure factor, $S(0)$, and the isothermal osmotic compressibility given by

$$S(0) = (k_B T/V) (\partial \Pi / \partial \phi)_T^{-1} \quad (13)$$

where V is the volume of the particles, and so we have

$$D(q \rightarrow 0) = [D_0 V / k_B T (\partial \Pi / \partial \phi)_T^{-1}] [1 + H(0)] \quad (14)$$

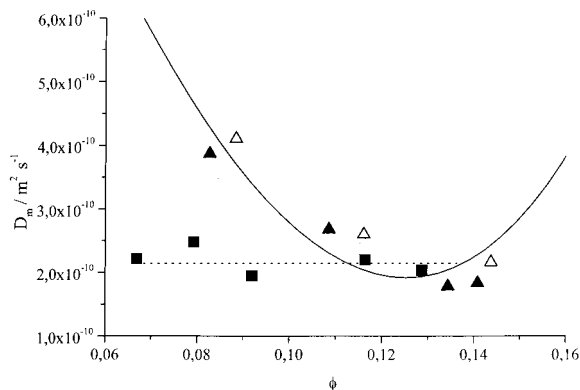


Figure 8. Variation of the apparent diffusion coefficient as a function of the droplet volume fraction of w/o microemulsions of AOT dissolved in toluene: squares $w_0 = 37$; filled triangles $w_0 = 40$; open triangles $w_0 = 45$. The line was calculated with eq 14.

TABLE 3: Temperature Effect on the Apparent Diffusion Coefficient and Hydrodynamic Radius of Microemulsions of AOT Dissolved in Toluene Containing Different Droplet Volume Fractions

ϕ	$T/$ (°C)	$D_m/$ $10^{10} \text{ m}^2/\text{s}$	$R_h^{\text{app}}/$ nm	ϕ	$T/$ (°C)	$D_m/$ $10^{10} \text{ m}^2/\text{s}$	$R_h^{\text{app}}/$ nm
0.083	21.1	3.11	1.1	0.109	39.6	3.69	1.1
0.083	25.4	3.58	1.0	0.134	25.2	1.78	2.0
0.083	38.5	4.98	0.8	0.134	27.5	1.91	1.9
0.083	48.5	6.27	0.7	0.134	31.7	2.05	1.9
0.109	22.5	2.40	1.5	0.134	37.8	2.33	1.8
0.109	25.1	2.68	1.3	0.134	42.4	2.78	1.6
0.109	26.8	2.80	1.3	0.134	44.5	2.90	1.5
0.109	30.5	3.03	1.3				

As in the case of the intensity data, we compute the osmotic compressibility using the Carnahan–Starling osmotic pressure, eq 6, together with an attractive term, eq 7. Figure 8 shows the experimental diffusion coefficient data obtained for microemulsions with $w_0 \geq 37$ along with the best fit of these data to eqs 6, 7, and 14, where the hydrodynamic term is neglected. The attractive parameter, A , found from the fit -20 ± 2 is in agreement with the one obtained from the intensity data, whereas the D_0 value $(4.5 \pm 0.5) \cdot 10^{-10} \text{ m}^2 \text{ s}^{-1}$ suggests that in this w_0 range droplets become smaller, and this unexpected result should be taken with precaution and more experimental results with more direct techniques such as PFG-NMR are needed in order to reach a conclusion.

An interesting consideration is derived from the fact that both DLS and SLS results can be analyzed as a function of the volume fraction independently of the w_0 value, and at each of the w_0 regimes, this implies that there should not be a significant difference between the microemulsion size within each of the water content regimes discussed above. This fact has been elsewhere observed in AOT w/o microemulsions dissolved in *n*-hexane, *n*-heptane, *n*-octane, and isooctane.¹⁶ In these microemulsions, the gyration radius shows no variation with w_0 at different water concentration regions. The location of this region changes with the solvent hydrocarbon chain length.

Effect of the Temperature. To compare the conductivity and light scattering results, we have also studied the effect of temperature on the diffusion coefficient for microemulsions containing the same water concentration, $w_0 = 40$, and different droplet volume fractions. The diffusion coefficients and the apparent hydrodynamic radius are collected in Table 3. A weak dependence of these parameters with temperature is observed; from Arrhenius-like plots ($\ln D_m$ vs $1/T$), the activation energy for droplet translation has been obtained for each ϕ value, Table 1.

Data in Table 1 show a slight dependence with ϕ as compared to the activation energy from conductivity and are always lower than those obtained by conductivity measurements. Differences can be due to differences in the phenomenon observed. Accordingly, to the charge fluctuation model,³¹ E_A from conductivity is related with the migration of charged aqueous droplets, whereas E_A from light scattering is related with translation movements of droplets. So, from results obtained in this work, the energy required to the migration of charge between droplets is greater than that needed to the translation of the microemulsions in the bulk solution.

It is interesting to notice that the energy of activation from conductivity sharply decreases for w/o microemulsions containing a droplet volume fraction $\phi = 0.134$, which correspond to the maximum of the light scattering intensity.

Conclusions

We use the electrical conductivity and light scattering measurements to study the effect of the droplet volume fraction on the size of AOT/toluene w/o microemulsions. The water and the surfactant concentrations were systematically modified from $w_0 = 15$ –50 and between 0.05 and 0.15 M, respectively. In addition, the effect of temperature was also studied.

Static and dynamic light scattering results showed two different behaviors corresponding to aggregates with small water concentration, $15 \leq w_0 \leq 35$, and with high water concentration, $w_0 > 37$. For aggregates with small water concentration, $15 \leq w_0 \leq 35$, dilute w/o microemulsions of hydrodynamic radius $R_h \approx 2.2$ nm are observed.

Results found in this work showed that attractive interactions between droplets become important in w/o microemulsions containing $w_0 > 37$. In this range of water concentration, the scattering intensity and the apparent diffusion coefficient at various droplet volume fractions are analyzed with a simple model involving the Carnahan–Starling hard-sphere model modified for an attractive interaction term. From the apparent diffusion coefficients at various droplet volume fractions for microemulsions with high water content, we found a diffusion coefficient at infinite dilution $D_0 = (4.5 \pm 0.5) 10^{-10} \text{ m}^2 \text{ s}^{-1}$. This value is greater than that for dilute w/o microemulsions, $(1.8 \pm 0.1) 10^{-10} \text{ m}^2 \text{ s}^{-1}$.

Finally, no percolation threshold is detected in the whole range of droplet volume fraction and temperature used in this work.

Acknowledgment. The authors acknowledge Junta de Castilla y León and Fondo Social Europeo for financial support of this project (SA04/99) and Servicio de Espectroscopía Raman-Rayleigh of the Universidad Complutense de Madrid for making available the light-scattering facility.

References and Notes

- Ueda, M.; Schelly, Z. A. *Langmuir* **1988**, *4*, 653.
- Hilfiker, R.; Eicke, H.-F.; Geiger, J.; Furler, G. *J. Colloid Interface Sci.* **1985**, *105*, 378.
- Fletcher, P. D. I.; Robinson, B. H.; Tabony, J. *J. Chem. Soc., Faraday Trans. 1* **1986**, *82*, 2311.
- Bruno, P.; Coselli, M.; Luisi, P. L.; Maestro, M.; Traini, A. *J. Phys. Chem.* **1990**, *94*, 5908.
- Oldfield, C.; Robinson, B. H.; Freedman, R.; *J. Chem. Soc., Faraday Trans. 1* **1990**, *86*, 833.
- Martin, C. A.; Magid, L. J. *J. Phys. Chem.* **1981**, *85*, 3938.
- Eicke, H.-F. *Pure Appl. Chem.* **1980**, *52*, 1349.
- Day, R. A.; Robinson, B. H.; Clarke, J. H. R.; Doherty, J. V. *J. Chem. Soc., Faraday Trans. 1* **1979**, *75*, 132.
- González-Blanco, C.; Rodríguez, L. J.; Velázquez, M. M. *J. Colloid Interface Sci.* **1999**, *211*, 380.
- González-Blanco, C.; Rodríguez, L. J.; Velázquez, M. M. *Langmuir* **1997**, *13*, 1938.
- González-Blanco, C.; Velázquez, M. M.; Costa, S. M. B.; Barreleiro, P. *J. Colloid Interface Sci.* **1997**, *189*, 43.
- González-Blanco, C.; Velázquez, M. M.; Ortega, F. *Langmuir* **1997**, *13*, 6095.
- González-Blanco, C.; Velázquez, M. M.; Costa, S. M. B.; Laia, C. A. T.; Medeiros, G. M. M. Manuscript in preparation.
- Kitahara, A.; Kobayashi, T.; Tachibana, T. *J. Chem. Soc.* **1962**, 363.
- Hirai, M.; Kawai-Hirai, R.; Yabuki, S.; Takizawa, T.; Hirai, T.; Kobayashi, K.; Amemiya, Y.; Oya, M. *J. Phys. Chem.* **1995**, *99*, 6652.
- Hirai, M.; Kawai-Hirai, R.; Sanada, M.; Iwase, H.; Mitsuya, S. *J. Phys. Chem. B* **1999**, *103*, 9658.
- Li, X.; Loong, C. K.; Thiyagarajan, P.; Lager, G. A.; Miranda, R. *J. Appl. Cryst.* **2000**, *33*, 628.
- Geiger, S.; Mandel, M. *J. Phys. Chem.* **1989**, *93*, 4195.
- Menger, F. M.; Yamada, K. *J. Am. Chem. Soc.* **1979**, *101*, 6731.
- Lin, J. E.; Zwolenik, J. J.; Fuoss, R. M. *J. Am. Chem. Soc.* **1959**, *81*, 1557.
- Koppel, D. E. *J. Chem. Phys.* **1972**, *57*, 4814.
- Handbook of Chemistry and Physics*, 60th ed.; CRC press: Boca Raton, FL, 1980.
- Eicke, H.-F. In *Microemulsions*; Robb, I. D., Ed.; Plenum Press: New York, 1982.
- Borkovec, M.; Eicke, H.-F.; Hammerick, H.; Das-Gupta, B. *J. Phys. Chem.* **1988**, *92*, 206.
- Cazabat, A. M.; Chateney, D.; Langevin, D.; Meunier, J. *Faraday Discuss. Chem. Soc.* **1982**, *76*, 291.
- Eicke, H.-F.; Denss, A. In *Solution Chemistry of Surfactants*; Mittal, K.-L., Ed.; Plenum Press: New York, 1979.
- Bhattacharya, S.; Skokes, J. P.; Kim, M. W.; Huang, J. *J. Phys. Rev. Lett.* **1985**, *55*, 1884.
- Bisal, S. R.; Bhattacharya, P. K.; Moulik, S. P. *J. Phys. Chem.* **1990**, *94*, 350.
- Mathew, C.; Patanjali, P. K.; Nabi, A.; Mitra, A. N. *Colloids Surf.* **1988**, *30*, 253.
- Kim, M. W.; Huang, J. S. *Phys. Rev. A* **1986**, *34*, 719.
- Eicke, H.-F.; Borkovec, M.; Das-Gupta, B. *J. Phys. Chem.* **1989**, *93*, 314.
- González-Blanco, C. Unpublished results.
- Alexandrov, Y.; Kozlovich, N.; Feldman, Y.; Texter, J. *J. Chem. Phys.* **1999**, *111*, 7023.
- Ray, S.; Paul, S.; Moulik, S. P. *J. Colloid Interface Sci.* **1996**, *183*, 6.
- Mukhopadhyay, L.; Bhattacharya, P. K.; Moulik, S. P. *Colloids Surf.* **1990**, *50*, 295.
- Eicke, H.-F.; Meier, W.; Hammerick, H. *Langmuir* **1994**, *10*, 2223.
- Moulik, S. P.; De, G. G.; Bhowmik, B. B.; Panda, A. K. *J. Phys. Chem. B* **1999**, *103*, 7122.
- Goodstein, D. In *States of Matter*; Prentice Hall: New York, 1975.
- Ortega, F.; Bacaluglu, R.; McKenzie, D. C.; Bunton, C. A.; Nicoli, D. F. *J. Chem. Phys.* **1990**, *94*, 501.
- Cazabat, M. A.; Langevin, D. *J. Chem. Phys.* **1981**, *74*, 3148.
- Calje, A. A.; Agterof, W. G. M.; Vrij, A. *Micellization, Solubilization and Microemulsions*; Plenum Press: New York, 1977.
- Berne, B. J.; Pecora, R. *Dynamic Light Scattering*; Wiley: New York, 1976.
- Ackerson, B. J. *J. Chem. Phys.* **1976**, *64*, 242; **1978**, *69*, 684.
- Pusey, P. N.; Tough, R. J. A. In *Dynamic Light Scattering and Velocimetry: Applications of Photon Correlation Spectroscopy*; Pecora, R., Ed.; Plenum Press: New York, 1985.